Inorg. Chem. **2008**, *47*, 10674−10681

Slow Magnetic Relaxation of a Ferromagnetic Ni^{II}_5 Cluster with an $S = 5$ Ground State

Athanassios K. Boudalis,*,† Michael Pissas,† Catherine P. Raptopoulou,† Vassilis Psycharis,† Belén Abarca,‡ and Rafael Ballesteros‡

Institute of Materials Science, NCSR "Demokritos", 153 10 Aghia Paraskevi Attikis, Greece, and Departamento de Química Orgánica, Faculdad de Farmacia, Universidad de Valencia, Avda. Vicente Andrés Estellés s/n, 46100 Burjassot (Valencia), Spain

Received July 31, 2008

Complex $[Ni_5\{pyCOpyC(O)(OMe)py\}_2(O_2CMe)_4(N_3)_4(MeOH)_2]\cdot 2MeOH\cdot 2.6H_2O$ (**1**$\cdot 2MeOH\cdot 2.6H_2O$) was synthesized by the reaction of $Ni(O_2CMe)_2\cdot 4H_2O$ with pyCOpyCOpy and NaN_3 in refluxing MeOH. It crystallizes in the monoclinic *C*2/*c* space group and consists of five Ni^{II} atoms in a helical arrangement. Direct current magnetic susceptibility studies reveal ferromagnetic interactions between the Ni^{II} ($S = 1$) ions, stabilizing an $S = 5$ ground state. Alternating current susceptibility experiments revealed the existence of out-of-phase signals indicative of slow magnetic relaxation. Analysis of the signals showed that they are composite, suggesting more than one relaxation process, while analysis of their magnitudes suggests not all molecules undergo slow magnetic relaxation. Magnetization field-sweep experiments revealed hysteresis at 1.8 K, and magnetization decay experiments clearly verified the appearance of slow magnetic relaxation at that temperature.

Introduction

Recent years have witnessed an impressive growth in the study of molecular magnetic materials. These materials exhibit interesting new magnetic phenomena, such as single-molecule magnetism (SMM)[1] and quantum tunneling of the magnetization (QTM),[2] which test the limits of current models for magnetism of condensed matter. Besides their theoretical interest, they have been proposed as potential candidates for various technological applications such as qubits for quantum computing,[3] coolants for magnetic refrigeration,[4] and MRI contrast agents.[5]

Because the structure−property relations for molecular magnetic materials are still very elusive, there is a constant need for new structures, belonging to the same structural type, and for new structural types for us to study. Given the nature of this chemistry, which is based on the interaction of metal ions with organic or inorganic ligands, the proper choice of such ligands may provide us with the new structural types desired. Our previous studies on the chemistry of the ligand $(py)_2CO$ (di-2-pyridyl ketone, dpk) showed that its carbonyl function can undergo metal-assisted solvolysis to yield its hemiacetal form in the case of alcoholic solvents or its *gem*-diol form in the case of nonalcoholic solvents. Subsequent deprotonations of these forms give rise to a rich coordination chemistry,[6] which has yielded polynuclear complexes with interesting properties.[7] Inspired by the chemistry of this ligand, we have previously started exploring the coordination chemistry of the ligand pyCOpyCOpy[8] [2,6-di-(2-pyridylcarbonyl)-pyridine, dpcp] shown in Scheme 1. Our synthetic endeavors, which have already afforded a Co^{II}_{20}

* To whom correspondence should be addressed. E-mail: tbou@ims.demokritos.gr. Tel: (+30) 210-6503346. Fax: (+30) 210-6503365.
† NCSR "Demokritos".
‡ Universidad de Valencia.

(1) (a) Christou, G.; Gatteschi, D.; Hendrickson, D. N.; Sessoli, R. *MRS Bull.* **2000**, *25*, 66. (b) Gatteschi, D.; Sessoli, R. *Angew. Chem., Int. Ed.* **2003**, *42*, 268.
(2) (a) Friedman, J. R.; Sarachik, M. P.; Tejada, J.; Ziolo, R. *Phys. Rev. Lett.* **1996**, *76*, 3830. (b) Thomas, L.; Lionti, F.; Ballou, R.; Gatteschi, D.; Sessoli, R.; Barbara, B. *Nature* **1996**, *383*, 145–147.
(3) (a) Leuenberger, M. N.; Loss, D. *Nature* **2001**, *410*, 789. (b) Hill, S.; Edwards, R. S.; Aliaga-Alcalde, N.; Christou, G. *Nature* **2003**, *302*, 1015. (c) Lehmann, J.; Gaita-Ariño, A.; Coronado, E.; Loss, D. *Nat. Nanotechnol.* **2007**, *2*, 312.
(4) Evangelisti, M.; Luis, F.; de Jongh, L. J.; Affronte, M. *J. Mater. Chem.* **2006**, *16*, 2534.
(5) Cage, B.; Russek, S. E.; Shoemaker, R.; Barker, A. J.; Stoldt, C.; Ramachandaran, V.; Dalal, N. S. *Polyhedron* **2007**, *26*, 2413.
(6) Papaefstathiou, G. S.; Perlepes, S. P. *Comments Inorg. Chem.* **2002**, *23*, 249.
(7) Boudalis, A. K.; Sanakis, Y.; Clemente-Juan, J. M.; Donnadieu, B.; Nastopoulos, V.; Mari, A.; Coppel, Y.; Tuchagues, J.-P.; Perlepes, S. P. *Chem.—Eur. J.* **2008**, *14*, 2514.
(8) Abarca, B.; Ballesteros, R.; Elmasnaouy, M. *Tetrahedron* **1998**, *54*, 15287.

10.1021/ic801441d CCC: $40.75
Published on Web 10/17/2008

Scheme 1. Ligands dpk [$(py)_2CO$] and dpcp (pyCOpyCOpy)

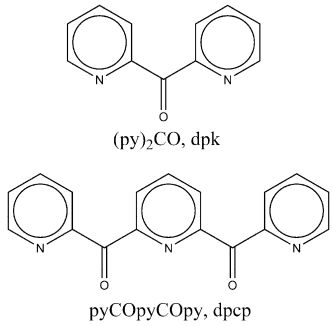

cluster showing slow magnetic relaxation,[9] a Cu^{II}_5[10] cluster, and two ferromagnetic Cu^{II}_4 and Co^{II}_4 clusters,[11] have confirmed this ligand's potential for interesting new structures and spin topologies. Following our studies with this ligand, we present our first studies of its Ni^{II} chemistry. Herein, we report on the synthesis and magnetic properties of the ferromagnetic $[Ni_5\{pyCOpyC(O)(OMe)py\}_2(O_2CMe)_4(N_3)_4(MeOH)_2]$ (**1**) cluster. Direct current (dc) and alternating current (ac) magnetic susceptibility studies, along with field-sweep and magnetization decay experiments, have been used to probe the static and dynamic magnetic properties of **1**.

Experimental Section

Materials. All materials were commercially available and used as received except dpcp, which was described according to a literature procedure.[8] **Caution!** *Azide salts are potentially explosive and should be handled with care and in small quantities.*

Synthesis. Solid dpcp (50.0 mg, 0.173 mmol) was added to a solution of $Ni(O_2CMe)_2\cdot 4H_2O$ (172 mg, 0.691 mmol) in MeOH (30 mL). The solution changed from light green to a darker green-brown color. Solid NaN_3 (45.0 mg, 0.691 mmol) was then added to the solution, which was heated to reflux for ~30 min. After cooling, the solution was layered with double the volume of Et_2O/*n*-hexane (1:1, v/v). Green-brown crystals of $\mathbf{1}\cdot 2MeOH\cdot 2.6H_2O$ formed after 2 days. These were collected by decantation of the mother liquor, washed with 4 × 5 mL of Et_2O, and dried in vacuo over silica gel. The yield was 0.097 g (~80% with respect to dpcp). The dried complex was analyzed as solvent free. Elemental analysis (%) calcd for $C_{46}H_{48}N_{18}Ni_5O_{16}$: C 39.39, H 3.45, N 17.98. Found: C 39.27, H 3.57, N 17.75. IR (KBr disk): υ = 2065 (vs) [$\upsilon_{as}(N_3)$], 1672 (m) [$\upsilon(C{=}O_{dpcp})$], 1563 (vs) [$\upsilon_{as}(COO)$], 1428 (vs) [$\upsilon_s(COO)$], 1321 (m), 1060 (m), 757 (w) [$\delta(C{-}H_{py})$], 682 (m) [$\pi(C{-}H)_{py}$] cm^{-1}.

X-ray Crystallography. A green-brown dichroic crystal of **1** with approximate dimensions of 0.20 × 0.30 × 0.65 mm was mounted in a capillary. Diffraction measurements were made on a Rigaku R-AXIS SPIDER Image Plate diffractometer using graphite monochromated Mo Kα radiation. Data collection (ω-scans) and processing (cell refinement, data reduction, and empirical absorption correction) were performed using the CrystalClear program package.[12] Important crystal data and parameters for data collection are reported in Table 1. The structure was solved by direct methods using SHELXS-97[13] and refined by full-matrix least-squares techniques on F^2 with SHELXL-97.[14] Further experimental crystallographic details for **1** are as follows: $2\theta_{max}$ = 50°; reflections collected/unique/used, 21011/6394 (R_{int} = 0.0439)/6394; 431 parameters refined; $(\Delta/\sigma)_{max}$ = 0.004; $(\Delta\rho)_{max}/(\Delta\rho)_{min}$ = 0.546/−0.327 e/Å^3; and R1/wR2 (for all data), 0.0507/0.1124. All hydrogen atoms were introduced at calculated positions as riding on bonded atoms. All non-hydrogen atoms were refined anisotropically except those of the solvate molecules, which were refined isotropically.

Table 1. Crystallographic Data for Complex $\mathbf{1}\cdot 2MeOH\cdot 2.6H_2O$

	$\mathbf{1}\cdot 2MeOH\cdot 2.6H_2O$
formula	$C_{48}H_{61.2}N_{18}Ni_5O_{20.6}$
fw	1513.50
cryst syst	monoclinic
space group	*C*2/*c*
T, K	298
λ, Å	Mo Kα (0.71073 Å)
a, Å	15.9095(6)
b, Å	21.7322(8)
c, Å	22.3558(7)
β, deg	108.2480(10)
V, Å^3	7340.8(4)
Z	4
ρ_{calcd}, g cm^{-3}	1.369
μ, mm^{-1}	1.333
R1[a]	0.0391[b]
wR2[a]	0.1039[b]

[a] $w = 1/[\sigma^2(F_o^2) + (aP)^2 + bP]$ and $P = (\max)(F_o^2,0) + (2F_c^2)/3$; R1 $= \sum(|F_o| - |F_c|)/\sum(|F_o|)$ and wR2 $= \{\sum[w(F_o^2 - F_c^2)^2]/\sum[w(F_o^2)^2]\}^{1/2}$. [b] For 5194 reflections with $I > 2\sigma(I)$.

Physical Measurements. Elemental analysis for carbon, hydrogen, and nitrogen was performed on a PerkinElmer 2400/*II* automatic analyzer. Infrared spectra were recorded as KBr pellets in the range of 4000−400 cm^{-1} on a Bruker Equinox 55/S FT-IR spectrophotometer. Variable temperature magnetic susceptibility measurements were carried out on a powdered sample of **1** in the 2−300 K temperature range using a QuantumDesign MPMS SQUID susceptometer operating under magnetic fields of 1, 5, 10, 25, and 50 kG. Magnetization isotherms between 0 and 5.5 T were collected at 2 K, and magnetic hysteresis experiments between ±5 T were carried out at 1.8 K. Alternating current susceptibility measurements were carried out on a QuantumDesign PPMS with ac magnetic field frequencies between 11 and 8111 Hz under a zero static magnetic field. Diamagnetic corrections for the complexes were estimated from Pascal's constants. The magnetic susceptibility for **1** has been computed by exact calculation of the energy levels associated with the spin Hamiltonian through diagonalization of the full matrix with a general program for axial symmetry.[15] Least-squares fittings were accomplished with an adapted version of the function-minimization program MINUIT.[16] The error factor *R* is defined as $R = \sum(\chi_{exp} - \chi_{calc})^2/N\chi_{exp}^2$, where *N* is the number of experimental points.

Results and Discussion

Synthesis. The reaction of dpcp with 4 equiv of $Ni(O_2CMe)_2\cdot 4H_2O$ and 4 equiv of NaN_3 in refluxing MeOH

(9) Boudalis, A. K.; Raptopoulou, C. P.; Abarca, B.; Ballesteros, R.; Chadlaoui, M.; Tuchagues, J.-P.; Terzis, A. *Angew. Chem., Int. Ed.* **2006**, *45*, 432.
(10) Boudalis, A. K.; Raptopoulou, C. P.; Psycharis, V.; Sanakis, Y.; Abarca, B.; Ballesteros, R.; Chadlaoui, M. *Dalton Trans.* **2007**, 3582.
(11) Boudalis, A. K.; Raptopoulou, C. P.; Psycharis, V.; Abarca, B.; Ballesteros, R. *Eur. J. Inorg. Chem.* **2008**, 2820.
(12) *CrystalClear*; Rigaku/MSC, Inc.: The Woodlands, TX, 2005.
(13) Sheldrick, G. M. *SHELXS-97: Structure Solving Program*; University of Göttingen: Göttingen, Germany, 1997.
(14) Sheldrick, G. M. *SHELXL-97: Crystal Structure Refinement Program*; University of Göttingen: Göttingen, Germany, 1997.
(15) Clemente-Juan, J.-M.; Mackiewicz, C.; Verelst, M.; Dahan, F.; Bousseksou, A.; Sanakis, Y.; Tuchagues, J.-P. *Inorg. Chem.* **2002**, *41*, 1478.
(16) James, F.; Roos, M. *Comput. Phys. Commun.* **1975**, *10*, 345.

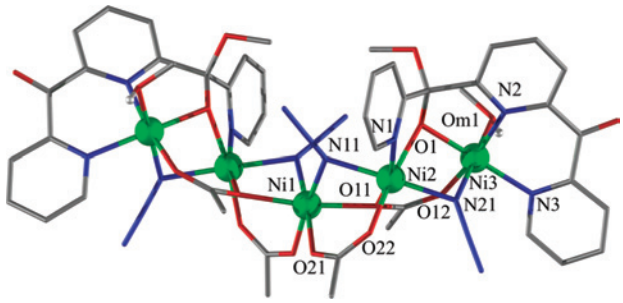

Figure 1. Partially labeled POV-Ray plot of **1** with thermal ellipsoids at the 30% probability level. Symmetry operation to generate equivalent atoms: $1 - x, y, 1.5 - z$.

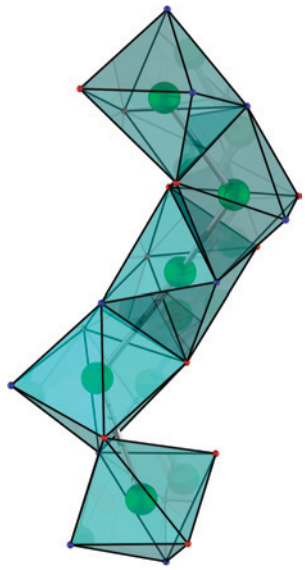

Figure 2. Helical arrangement of the five Ni^{II} atoms.

led to a green-brown solution, from which layering with Et_2O/*n*-hexane afforded green-brown crystals of $[Ni_5(L)_2(\mu\text{-}O_2CMe)_2(\mu_3\text{-}O_2CMe)_2(N_3)_4(MeOH)_2]\cdot 2.6MeO\cdot 2.6H_2O$ (**1**·2MeOH·2.6H_2O), where $L^- =$ pyCOpyC(O^-)(OMe)py. The reaction leading to the complex is summarized in eq 1.

$$5Ni(O_2CMe)_2\cdot 4H_2O + 2pyCOpyCOpy + 4NaN_3 + 4MeOH \xrightarrow[\Delta]{MeOH} \underset{\mathbf{1}}{[Ni_5\{pyCOpyC(O)(OMe)py\}_2(O_2CMe)_4(N_3)_4(MeOH)_2]} + 20H_2O + 2MeCO_2H + 4NaO_2CMe \quad (1)$$

It is noteworthy that despite the heating of the reaction mixture only one of the carbonyl functions of the dpcp ligand was alcoholyzed to yield the hemiacetal form of the ligand. Thus, the ligand is present in its carbonyl-hemiacetal form.

Description of the Structure. Complex **1** (Figure 1) is the first Ni^{II} complex with the dpcp ligand. It crystallizes in the monoclinic *C*2/*c* space group, and it contains five hexacoordinate Ni^{II} ions arranged in a helical fashion (Figure 2). Selected interatomic bond distances (Å) and angles (deg) are shown in Table S1 of the Supporting Information. To the best of our knowledge, this is the first Ni_5 cluster in which the Ni atoms are found in a helical arrangement.

Ni(1) sits on a 2-fold axis through which the two halves of the molecule are related. Bridging between each pair of nickel atoms is achieved through end-on azides: Ni(1)−Ni(2) through atom N(11) and Ni(2)−Ni(3) through atom N(21). Additional bridging is achieved through the acetato and the dpcp ligands. In particular, Ni(1) and Ni(2) are bridged by one *syn-syn* $\mu_2{:}\eta^1{:}\eta^1$ acetate and by the O(11) carboxylate oxygen of a *syn-syn-anti* $\mu_3{:}\eta^1{:}\eta^2$ carboxylate, which acts as a monatomic bridge. This latter carboxylate also acts as a μ_3 bridge between Ni(1), Ni(2), and Ni(3). Finally, Ni(2) and Ni(3) are bridged by the $\{pyCOpyC(O)(OMe)py\}^-$ ligand, which offers a monatomic alkoxo bridge through atom O(1).

Scheme 2. Crystallographically Established Coordination Mode of the dpcp Ligand in **1**

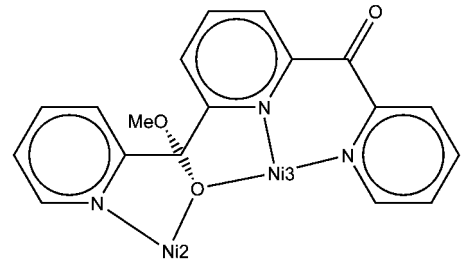

It is noteworthy that only one carbonyl function of the ligand has been alcoholyzed to the hemiacetal form, C(6), while the other has retained its carbonyl character, C(12), leading to the carbonyl-hemiacetal form of the ligand (Scheme 2). This form has only occurred in mononuclear complexes,[17] and this is its first occurrence as a bridge in a polynuclear complex.

The molecules of **1** are well separated from each other with the closest intramolecular Ni···Ni distance being ~8.0 Å between Ni(3) (x, y, z) and Ni(3) ($1.5 - x, 0.5 - y, 1 - z$).

Static Magnetic Properties. The $\chi_M T$ product of **1** (1 T at 300 K) is 7.34 $cm^3\ mol^{-1}$ K (Figure 3) above the value predicted for five noninteracting $S = 1$ ions (6.05 $cm^3\ mol^{-1}$ K, $g = 2.2$), suggesting ferromagnetic interactions. This is corroborated by the increase of the $\chi_M T$ value upon cooling to a maximum of 15.86 $cm^3\ mol^{-1}$ K at 16 K. This maximum is field dependent and shifts to higher temperatures at higher magnetic fields, while its value decreases. Data collected at various fields, from zero magnetic field (ac data) to 5 T, converge to the same values above ~75 K. For the interpretation of these data, a simple model accounting for nearest-neighbor interactions was used, while terms to account for the single-ion axial zero-field splittings of the Ni^{II} ions and the Zeeman splittings inside the magnetic field were also introduced. Because of the symmetry of the molecule as revealed by X-ray crystallography, it was assumed that $J_{23} = J_{2'3'} = J_1$ and $J_{12} = J_{1'2'} = J_2$; in order to avoid overparametrization of our problem, a global single-ion zero-field splitting (zfs) parameter, D, was used for all Ni^{II} ions. The respective spin Hamiltonian is given in eq 2.

(17) Chen, X.-D.; Du, M.; He, F.; Chen, X.-M.; Mak, T. C. W. *Polyhedron* **2005**, *24*, 1047–1053.

$$\hat{H} = -2[J_1(\hat{\mathbf{S}}_2\hat{\mathbf{S}}_3 + \hat{\mathbf{S}}_{2'}\hat{\mathbf{S}}_{3'}) + J_2(\hat{\mathbf{S}}_1\hat{\mathbf{S}}_2 + \hat{\mathbf{S}}_1\hat{\mathbf{S}}_{2'}) + D\sum_{i=1}^{5} S_{i,z}^2 + g\mu_B\mathbf{H}\sum_{i=1}^{5}\hat{\mathbf{S}}_i \quad (2)$$

Initial fitting attempts were carried out on data collected at low fields, which gave poor results. In the high-temperature region, the experimental data were well reproduced, but at low temperatures they seriously underestimated the $\chi_M T$ values. It was found that this problem was less pronounced for the 1 T data set, where the quality of fit was marginally acceptable. For the data collected at 2.5 T and above, the results were of significantly higher quality. Thus, the 2.5 and 5 T data were simultaneously fitted to the Hamiltonian. Two solutions were derived, one for $D < 0$ and one for $D > 0$, with best-fit parameters: $J_1 = 19.7\ cm^{-1}$, $J_2 = 10.7\ cm^{-1}$, $D = -3.2\ cm^{-1}$, *and* $g = 2.22$ (solution **A**, $R = 2.7 \times 10^{-4}$) and $J_1 = 19.7\ cm^{-1}$, $J_2 = 10.7\ cm^{-1}$, $D = 3.5\ cm^{-1}$, *and* $g = 2.22$ (solution **B**, $R = 3.0 \times 10^{-4}$) both suggesting an $S = 5$ ground state. To verify the uniqueness of each solution for $D < 0$ or $D > 0$, error-contour plots were constructed in Figures S1 and S2, respectively, of the Supporting Information. These verified each of the solutions as the global minima, revealing another set of local minima (solution **C**: $J_1 = 7.4\ cm^{-1}$, $J_2 = 21.9\ cm^{-1}$, $D = -3.2\ cm^{-1}$, $g = 2.23$, and $R = 3.1 \times 10^{-4}$; solution **D**: $J_1 = 7.4\ cm^{-1}$, $J_2 = 21.8\ cm^{-1}$, $D = 3.6\ cm^{-1}$, $g = 2.23$, and $R = 3.4 \times 10^{-4}$), which were of lower quality. Solutions **A** and **B** are of relatively higher quality than **C** and **D**, although the sign of D does not greatly influence the quality of the fits. However, its magnitude is consistently in the $3.2-3.6\ cm^{-1}$ region. It is also noteworthy that all solutions, **A**−**D**, suggest an $S = 4$ excited state at $11.5-13.5\ cm^{-1}$ (i.e., relatively close to the ground state).

As a general observation, we may say that the spin Hamiltonian does not seem to be a valid approach for the low-field data of complex **1**, while it does becomes valid for data collected at higher fields. We suggest the origin of this behavior is the orbital contributions in Ni^{II} ions, which are significant. At low fields, the coupling between **L** and **S** may be strong enough for the Zeeman term to be considered as a perturbation. In this case, the coupled representation is more accurate; therefore, the spin-Hamiltonian approach is not valid. However, at sufficiently high fields the Zeeman term is more important and causes the system to revert to the uncoupled representation (Paschen−Back limit). In such a case, S and M_S become good quantum numbers, and the spin Hamiltonian is a valid approach.

The ferromagnetic interactions suggested by the fits are in line with the presence of end-on bridging azides between the Ni^{II} ions [Ni(1)−N(11)−Ni(2), 98.2°; Ni(2)−N(21)−Ni(3), 91.3°], which are known to promote ferromagnetic couplings. In addition, the Ni−O−Ni angles of the monatomic bridges provided by the carboxylato [Ni(1)−O(11)−Ni(2), 95.6°] and alkoxo [Ni(2)−O(1)−Ni(3), 95.0°] ligands are not too large to promote strong antiferromagnetic couplings.

The nature of the ground state was verified by isothermal magnetization studies at 2 K (Figure 4). The M versus H data indicate partial saturation near 5.5 T with a magnetization value of $\sim 11.10\ N_A\mu_B$. This agrees very well with the saturation magnetization of an $S = 5$ system ($11.06\ N_A\mu_B$, $g = 2.22$). M versus HT^{-1} data at low temperatures (2−8 K, Figure S2 of the Supporting Information) could not be fitted by assuming a well-isolated ground state, probably because of the presence of low-lying excited states (vide supra). However, from all of the possibilities examined, only an assumption of an $S = 5$ ground state yielded reasonable results. A small step that appears around 1 T is tentatively attributed to level crossings within the cluster, although the complexity of the spin system impedes us from performing reliable calculations to reproduce this behavior. A similar behavior had been observed in two enneanuclear SMMs previously reported by us.[7]

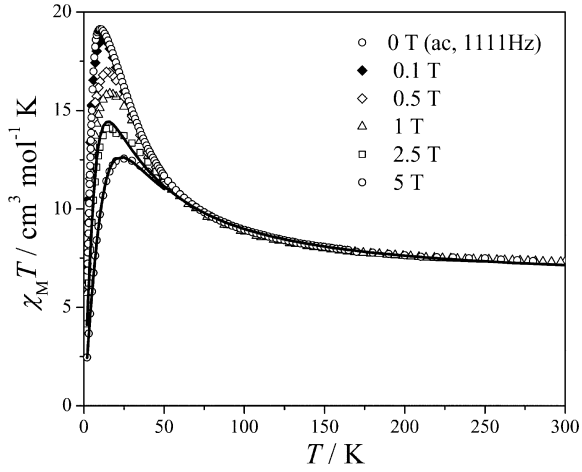

Figure 3. $\chi_M T$ versus T data for **1** under various applied fields, along with fits to the 2.5 and 5 T data (lines). The ac zero-field data were recorded under a magnetic field oscillating at 1111 Hz.

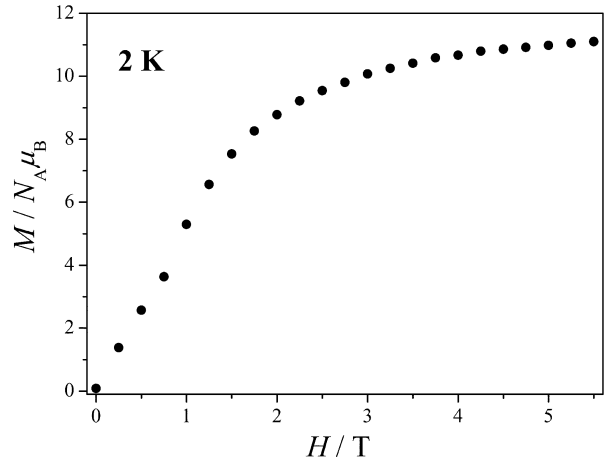

Figure 4. M versus H data for complex **1** at 2 K.

Dynamic Magnetic Properties. (i) Alternating Current Susceptibility Studies. Complex **1** was found to exhibit a high-spin ground state, along with a significant anisotropy of its Ni^{II} ions. These attributes are regarded as favorable for the observation of single-molecule magnetism, so magnetization relaxation experiments were undertaken to test this possibility. Indicative ac susceptibility experiments are shown in Figure 5. The magnetic susceptibility of **1** (2−13 K) was measured under a 10 G alternating magnetic field, oscillating

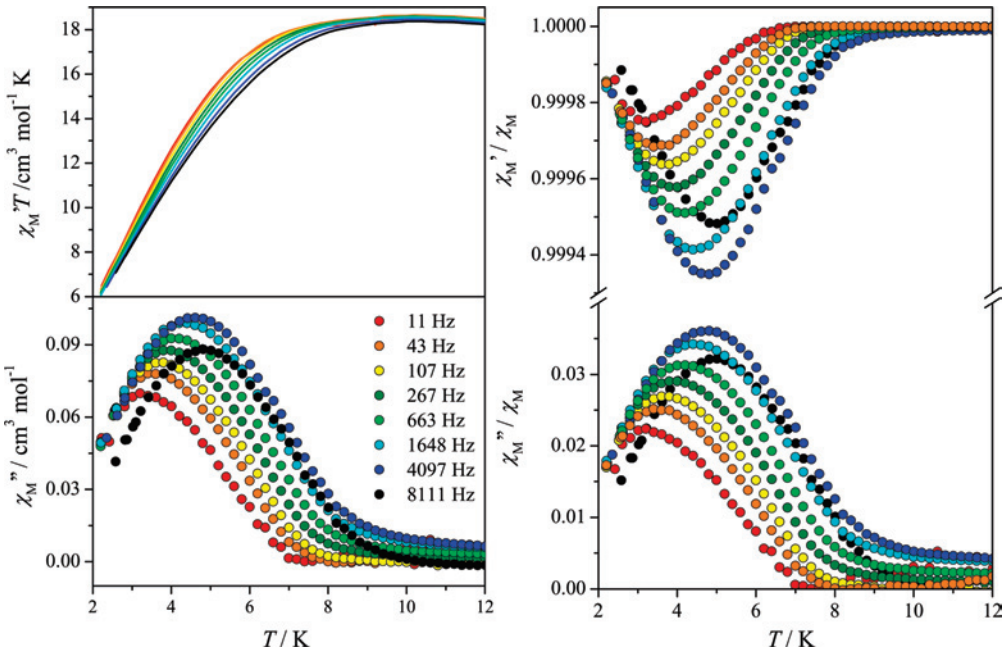

Figure 5. In-phase and out-of-phase ac susceptibility data for **1** at eight characteristic frequencies. Data are shown as $\chi_M'T$ versus T and χ_M'' versus T plots (left) and as χ_M'/χ_M versus T and χ_M''/χ_M versus T plots (right).

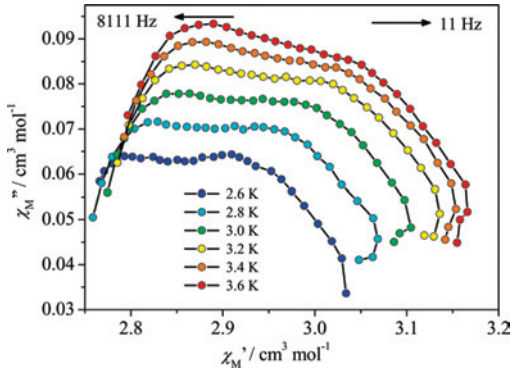

Figure 6. Cole−Cole plot for **1** between 2.6 and 3.6 K.

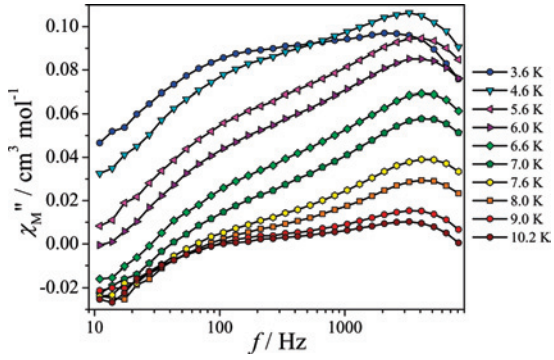

Figure 7. χ_M'' versus f plots for **1** at various temperatures.

at frequencies between 11 and 8111 Hz. Clear, frequency-dependent, out-of-phase signals were detected for all frequencies. These signals were manifested as clearly visible peaks well above 2 K (3.3 K at 11 Hz). It is noteworthy that to date, for all Ni^{II} clusters described as SMMs,[18] out-of-phase signals have not exhibited peaks above 2 K. The only other Ni^{II} cluster for which slow magnetic relaxation has been observed at higher temperatures (∼18 K) is a Ni^{II}_{10} complex,[19] which relaxes through a fundamentally different mechanism than that of SMMs.

(18) (a) Andres, H.; Basler, R.; Blake, A. J.; Cadiou, C.; Chaboussant, G.; Grant, C. M.; Güdel, H.-U.; Murrie, M.; Parsons, S.; Paulsen, C.; Semadini, F.; Villar, V.; Wernsdorfer, W.; Winpenny, R. E. P. *Chem.—Eur. J.* **2002**, *8*, 4867. (b) Ochsenbein, S. T.; Murrie, M.; Rusanov, E.; Stoeckli-Evans, H.; Sekine, C.; Güdel, H. U. *Inorg. Chem.* **2002**, *41*, 5133. (c) Young, E.-C.; Wernsdorfer, W.; Hill, S.; Edwards, R. S.; Nakano, M.; Maccagnano, S.; Zakharov, L. N.; Rheingold, A. L.; Christou, G.; Hendrickson, D. N. *Polyhedron* **2003**, *22*, 1727. (d) Yang, E.-C.; Wernsdorfer, W.; Zakharov, L. N.; Karaki, Y.; Yamaguchi, A.; Isidro, R. M.; Lu, G.-D.; Wilson, S. A.; Rheingold, A. L.; Ishimoto, H.; Hendrickson, D. N. *Inorg. Chem.* **2006**, *45*, 529. (e) Moragues-Cánovas, M.; Helliwell, M.; Ricard, L.; Rivière, É.; Wernsdorfer, W.; Brechin, E. K.; Mallah, T. *Eur. J. Inorg. Chem.* **2004**, 2219. (f) Aromí, G.; Parsons, S.; Wernsdorfer, W.; Brechin, E. K.; McInnes, E. J. L. *Chem. Commun. (Cambridge, U.K.)* **2005**, 5038.

In order to use the out-of-phase data to determine the relaxation parameters of **1**, we tried to fit the ac signals to Lorentzians in order to determine the peak maxima. However, a single Lorentzian could not reproduce the shape of the curves with two Lorentzians always being required. This asymmetry of the signals prompted us to examine if relaxation occurred through more than one relaxation time. Cole−Cole plots at various temperatures revealed the presence of a composite curve departing from the expected semicircle. This was clear evidence that at least two relaxation times govern the slow relaxation of **1**.

The same conclusion may be drawn from plots of χ_M'' versus f at several different temperatures. Whereas one single peak would be expected for a system relaxing through a single relaxation time, these plots revealed the presence of two broad and overlapping peaks (Figure 7). From inspection of these plots, characteristic time scales of $\sim 10^2$ and $\sim 10^4$ s are derived for the two relaxation processes.

Finally, another point should be made concerning the magnitude of the out-of-phase signals, χ_M. In the majority of the studies on SMMs, comments on the magnitudes of these signals are absent with the discussion being focused on the

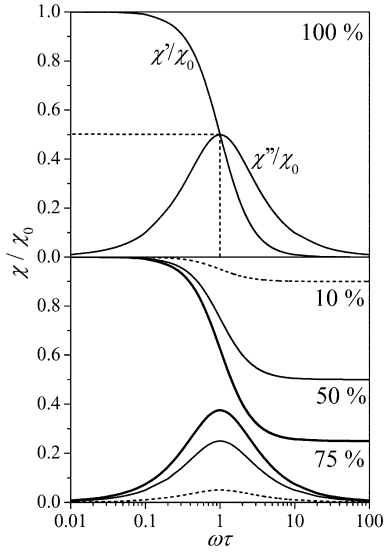

Figure 8. χ'/χ_0 and χ''/χ_0 ratios of the in-phase, χ', and out-of-phase, χ'', magnetic susceptibilities compared to the total magnetic susceptibility, χ_0, of a slowly relaxing system following Arrhenius kinetics. Curves corresponding to a system undergoing slow relaxation with 100% (top) or with smaller fractions (bottom) of the molecules are given for the in-phase and out-of-phase susceptibilities.

temperatures where these magnitudes arise and whether or not clear maxima are visible (see the discussion below for an indicative list of such SMM studies). The conclusions derived from these studies concern the dynamics of slow magnetic relaxation for the slowly relaxing molecules. However, the lack of a quantitative discussion on the magnitudes of these signals conceals the fact that often the condition of slow magnetic relaxation may not be fulfilled for all molecules.

For a slowly relaxing system moving through a single Arrhenius process with a time constant, τ, the magnetization will satisfy the relation $\tau\, dM/dt + M = 0$. It may be shown that the magnetic susceptibility of the system, χ_0, is related to its in-phase and out-of-phase components, $\chi'$and χ'', through the relations

$$\frac{\chi'}{\chi_0} = \frac{1}{1+(\omega\tau)^2} \tag{3}$$

and

$$\frac{\chi''}{\chi_0} = \frac{\omega\tau}{1+(\omega\tau)^2} \tag{4}$$

with $\omega = 2\pi f$, where f is the frequency of the oscillating magnetic field. As shown in Figure 8 (top), χ'' acquires its maximum value at $\omega\tau = 1$, which is equal to half of the total magnetic susceptibility. However, if only a fraction, ρ, undergoes slow relaxation, then the relations would transform to

$$\frac{\chi'}{\chi_0} = (1-\rho) + \rho\frac{1}{1+(\omega\tau)^2} \tag{5}$$

and

$$\frac{\chi''}{\chi_0} = \rho\frac{\omega\tau}{1+(\omega\tau)^2} \tag{6}$$

This would induce a decrease in the maximum χ_M''/χ_M value (Figure 8, bottom).

As we see, the χ_M''/χ_M ratio is an indicator of (i) whether a system undergoes relaxation through one or more processes

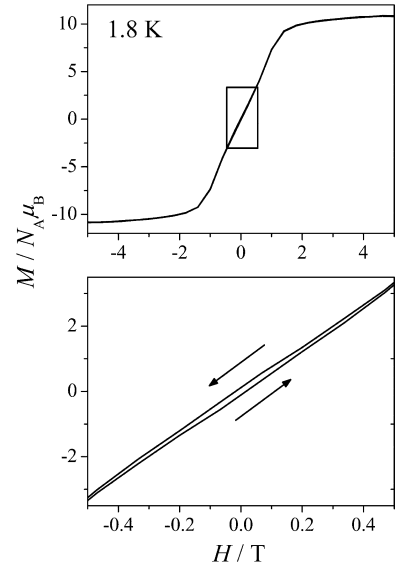

Figure 9. 1.8 K hysteresis loop of **1** between ±5 T (top) and between ±0.5 T (bottom).

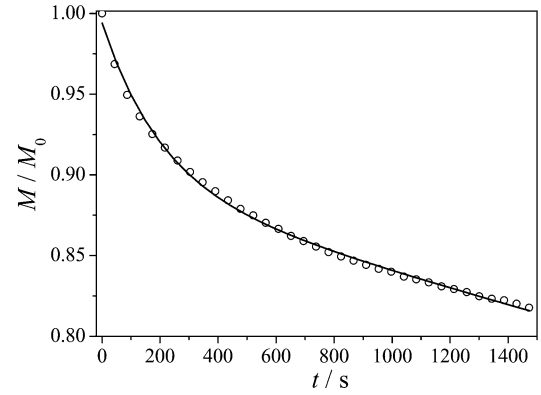

Figure 10. Magnetization decay of **1** at 1.8 K and zero magnetic field. The solid line is a fit to the data according to a process involving two relaxation times as described in the text.

(a single maximum indicating a single relaxation time, τ, and (ii) whether the whole sample undergoes relaxation or a fraction of it (maximum value of 0.5 when the whole sample undergoes relaxation). Behavior close to that expected for a single relaxation process and relaxation of the whole sample has been observed generally for the Mn_{12} family of SMMs and for $\{[Fe_8O_2(OH)_{12}(tacn)_6]Br_7\cdot H_2O\}Br\cdot H_2O$ (tacn = triazacyclononane),[20] $[Fe_4(OMe)_6(dpm)_6]$ (Hdpm = dipivaloylmethane),[21] $[CuL^1Tb(hfac)_2]_2$ [Hhfac = hexafluoroacetylacetone, H_3L^1 = 1-(2-hydroxybenzamido)-2-(2-hydroxy-3-methoxybenzylideneamino)-ethane],[22] $[\{Dy(hfac)_3\}_2\{Cu(dpko)_2\}]$ (Hdpko

(19) Carretta, S.; Santini, P.; Amoretti, G.; Affronte, M.; Candini, A.; Ghirri, A.; Tidmarsh, I. S.; Laye, R. H.; Shaw, R.; McInnes, E. J. L. *Phys. Rev. Lett.* **2006**, *97*, 207201.
(20) (a) Delfs, C.; Gatteschi, D.; Pardi, L.; Sessoli, R.; Wieghardt, K.; Hanke, D. *Inorg. Chem.* **1993**, *32*, 3099. (b) Barra, A.-L.; Debrunner, P.; Gatteschi, D.; Schulz, C. E.; Sessoli, R. *Europhys. Lett.* **1996**, *35*, 133.
(21) Barra, A. L.; Caneschi, A.; Cornia, A.; de Biani, F. F.; Gatteschi, D.; Sangregorio, C.; Sessoli, R.; Sorace, L. *J. Am. Chem. Soc.* **1999**, *121*, 5302.
(22) Osa, S.; Kido, T.; Matsumoto, N.; Re, N.; Pochaba, A.; Mrozinski, J. *J. Am. Chem. Soc.* **2004**, *126*, 420.

= di-2-pyridylketonoxime),[23] [{CuL^{1}Tb(*o*-van)(O_2CMe)(MeOH)}$_2$] (H*o*-van = 3-methoxysalicylaldehyde),[24] and [Dy(hfac)$_3$-{NITpPy}]$_2$ (NITpPy = 2-(4-pyridyl)-4,4,5,5-tetramethyl-4,5-dihydro-1H-imidazolyl-3-oxide)[25] to mention a few SMMs. However, we could not find any explicit references to the χ_M''/χ_M ratio of each sample. Our estimates have been based on visual comparison of the χ_M'' versus T curves with the $\chi_M T$, χ_M', or $\chi_M' T$ versus T curves, depending on which curves were reported. Thus, they are bound to be somewhat inaccurate, although still relevant. In one case, χ_M''/χ_M versus T curves were reported for the (^{n}Bu$_4$N)[Ln(Pc)$_2$] SMMs (Ln^{III} = Tb^{III}, Dy^{III}, H_2Pc = phthalocyanine)[26] for which the authors reported maxima of 0.35−0.40 (i.e., close to the ideal behavior). We estimated values close to ∼0.4 for [Fe(bpca)(μ-bpca)Dy(NO$_3$)$_4$] [Hbpca = bis(2-pyridylcarbonylamine)],[27] [(RTp)Fe(CN)$_3$Ni(tren)]$_2$(ClO$_4$)$_2$ [RTp = alkyltrispyrazolylborate, R = Ph, ^{i}Bu, tren = tris(2-amino)ethylamine],[28] and {[(pzTp)Fe^{III}(CN)$_3$]$_2$[Ni^{II}(bipy)$_2$]}.[29] For {[(Tp*)Fe^{III}(CN)$_3$]$_2$-[Ni^{II}(bipy)$_2$]$_2$[OTf]$_2$} (OTf$^-$ = trifluoromethanesulfonate),[30] [Mn$_{12}$-O$_8$Cl$_4$(O_2CPh)$_8$(hmp)$_6$] [Hhmp = 2-(hydroxymethyl)pyridine],[31] and [Mn$_{18}$O$_{14}$(O_2CMe)$_{18}$(hep)$_4$(Hhep)$_2$(H_2O)$_2$](ClO$_4$)$_2$ [Hhep = 2-(hydroxyethyl)pyridine],[32] we estimate the corresponding values at ∼0.3.

Intermediate cases include [Co(NCS)$_2$L$_4$],[33] [Mn$_6$O$_2$(Et-salox)$_6${O_2CPh(4-Me)}$_2$(EtOH)$_6$],[34] [Mn$_7$L$_6$] [H_3L = N-(2-hydroxy-5-nitrobenzyl)-iminodiethanol],[35] and [Mn$_9$O$_7$(O_2CMe)$_{11}$-(thme)(py)$_3$(H_2O)$_2$] [H_3thme = 1,1,1-tris(hydroxymethyl)ethane][36] (∼0.2−0.3).

On the other hand, SMMs with very low respective values have been reported. For [Fe$_9$(O_2CMe)$_8${(py)$_2$$CO_2$}$_4(NCO)_2$], a value of ∼0.15 was derived from the raw data available to us,[7] while values between 0.09 and 0.1 have been estimated for [Co(NCO)$_2$(4NOPy)$_4$],[37] [Et$_3$NH]$_2$[Mn$_{20}$O$_{12}$(OH)$_2$(O_3PCH$_2$Ph)$_{12}$-(O_2CCMe$_3$)$_{10}$(py)$_2$],[38] [Et$_3$NH][Co$_8$(chp)$_{10}$(O_3PPh)$_2$(NO$_3$)$_3$(Hchp)$_2$] (Hchp = 6-chloro-2-hydroxypyridine),[39] (Hpy)$_5$[Fe$_{13}$F$_{24}$(OMe)$_{12}$-O$_4$],[40] and [L^{1}CuTb(hfac)$_2$]$_2$.[41] Even lower values have been estimated for [(PY5Me$_2$)$_4$Mn$_4$Re(CN)$_7$](PF$_6$) [PY5Me$_2$ = 2,6-bis{1,1-bis(2-pyridyl)ethyl}pyridine] (∼0.07),[42] [Fe$_9$(O_2CMe)$_8$-{(py)$_2$$CO_2$}$_4$($N_3$)$_2$] (∼0.04, data available),[7] and [Ni{Ni(bipy)(H_2O)}$_8$-{W(CN)$_8$}$_6$][43] (∼0.01). We should note that we only report SMMs where the out-of-phase peaks were clearly observed; therefore, the maximum χ_M'' values are known.

In one study, van Slageren et al.[40] discussed the low χ_M'' value observed for (Hpy)$_5$[Fe$_{13}$F$_{24}$(OMe)$_{12}$O$_4$], attributing it to a slowly relaxing fraction of the molecules undergoing over-the-barrier relaxation with the rest undergoing fast under-the-barrier relaxation. Shortly thereafter, we reached similar conclusions, concerning the diferrous SMM [Fe$_2$(NCO)$_3$(acpypentO)] (HacpypentO = 1,5-bis{[2-pyridyl(1-ethyl)imino]}pentane-3-ol),[44] based on Mössbauer, EPR, and ac magnetic susceptibility data. In the case of complex **1**, the χ_M''/χ_M value does not overcome 0.036 (at 4.8 K for a 4097 Hz oscillating field). This would suggest that approximately 7.2% of the molecules undergo slow magnetic relaxation, assuming a single relaxation time.

(ii) Magnetization Hysteresis and Magnetization Decay Experiments. In order to better probe the slow magnetic relaxation properties, we conducted magnetization field-sweep experiments as well as magnetization decay experiments on our powdered sample. These experiments were conducted at 1.8 K, which is the lower limit of our instrument. In particular, field sweeps between ±1 T revealed a small but non-negligible hysteresis with a coercive field on the order of 350 G.

Magnetization decay was also indicative of slow magnetic relaxation. The sample was saturated at a 1 T field, while decay was monitored at a zero field. After saturation, the field was rapidly reduced to its final value (typically within ∼150 s), and the magnetization was measured at constant time intervals. The magnetization could not be fitted to a single relaxation time, and two relaxation times were required to satisfactorily fit the data:

$$M(t)/M_0 = Ae^{-t/\tau_1} + (1-A)e^{-t/\tau_2} \quad (7)$$

where τ_1 and τ_2 are the relaxation times of the two processes and A is the fraction for the process with relaxation time τ_1. Fitting of the data yielded values $A = 0.1$, $\tau_1 = 1.8 \times 10^2$ s, and $\tau_2 = 1.5 \times 10^5$ s. Small discrepancies between the

(23) Mori, F.; Nyui, T.; Ishida, T.; Nogami, T.; Choi, K.-Y.; Nojiri, H. *J. Am. Chem. Soc.* **2006**, *128*, 1440.
(24) Hamamatsu, T.; Yabe, K.; Towatari, M.; Matsumoto, N.; Re, N.; Pochaba, A.; Mrozinski, J. *Bull. Chem. Soc. Jpn.* **2007**, *80*, 523.
(25) Poneti, G.; Bernot, K.; Bogani, L.; Caneschi, A.; Sessoli, R.; Wernsdorfer, W.; Gatteschi, D. *Chem. Commun. (Cambridge, U.K.)* **2007**, 1807.
(26) Ishikawa, N.; Sugita, M.; Ishikawa, T.; Koshihara, S.; Kaizu, Y. *J. Am. Chem. Soc.* **2003**, *125*, 8694.
(27) Ferbinteanu, M.; Kajiwara, T.; Choi, K.-Y.; Nojiri, H.; Nakamoto, A.; Kojima, N.; Cimpoesu, F.; Fujimura, Y.; Takaishi, S.; Yamashita, M. *J. Am. Chem. Soc.* **2006**, *128*, 9008.
(28) Wang, C.-F.; Liu, W.; Song, Y.; Zhou, X.-H.; Zuo, J.-L.; You, X.-Z. *Eur. J. Inorg. Chem.* **2008**, 717.
(29) Li, D.; Clérac, R.; Parkin, S.; Wang, G.; Yee, G. T.; Holmes, S. M. *Inorg. Chem.* **2006**, *45*, 5251.
(30) Li, D.; Clérac, R.; Wang, G.; Yee, G. T.; Holmes, S. M. *Eur. J. Inorg. Chem.* **2007**, 1341.
(31) Boskovic, C.; Brechin, E. K.; Streib, W. E.; Folting, K.; Hendrickson, D. N.; Christou, G. *Chem. Commun. (Cambridge, U.K.)* **2001**, 467.
(32) Brechin, E. K.; Sañudo, E. C.; Wernsdorfer, W.; Boskovic, C.; Yoo, J.; Hendrickson, D. N.; Yamaguchi, A.; Ishimoto, H.; Concolino, T. E.; Rheingold, A. L.; Christou, G. *Inorg. Chem.* **2005**, *44*, 502.
(33) Karasawa, S.; Zhou, G.; Morikawa, H.; Koga, N. *J. Am. Chem. Soc.* **2003**, *125*, 13676.
(34) Milios, C. J.; Inglis, R.; Bagai, R.; Wernsdorfer, W.; Collins, A.; Moggach, S.; Parsons, S.; Perlepes, S. P.; Christou, G.; Brechin, E. K. *Chem. Commun. (Cambridge, U.K.)* **2007**, 3476.
(35) Koizumi, S.; Nihei, M.; Nakano, M.; Oshio, H. *Inorg. Chem.* **2005**, *44*, 1208.
(36) Brechin, E. K.; Soler, M.; Davidson, J.; Hendrickson, D. N.; Parsons, S.; Christou, G. *Chem. Commun. (Cambridge, U.K.)* **2002**, 2252.
(37) Kanegawa, S.; Karasawa, S.; Nakano, M.; Koga, N. *Chem. Commun. (Cambridge, U.K.)* **2004**, 1750.
(38) Maheswaran, S.; Chastanet, G.; Teat, S. J.; Mallah, T.; Sessoli, R.; Wernsdorfer, W.; Winpenny, R. E. P. *Angew. Chem., Int. Ed.* **2005**, *44*, 5044.
(39) Langley, S. J.; Helliwell, M.; Sessoli, R.; Rosa, P.; Wernsdorfer, W.; Winpenny, R. E. P. *Chem. Commun. (Cambridge, U.K.)* **2005**, 5029.
(40) van Slageren, J.; Rosa, P.; Caneschi, A.; Sessoli, R.; Casellas, H.; Rakitin, Y. V.; Cianchi, L.; Del Giallo, F.; Spina, G.; Bino, A.; Barra, A.-L.; Guidi, T.; Carretta, S.; Caciuffo, R. *Phys. Rev.* **2006**, *B73*, 014422.
(41) Hamamatsu, T.; Yabe, K.; Towatari, M.; Osa, S.; Matsumoto, N.; Re, N.; Pochaba, A.; Mrozinski, J.; Gallani, J.-L.; Barla, A.; Imperia, P.; Paulsen, C.; Kappler, J.-P. *Inorg. Chem.* **2007**, *46*, 4458.
(42) Freedman, D. E.; Jenkins, D. M.; Iavarone, A. T.; Long, J. R. *J. Am. Chem. Soc.* **2008**, *130*, 2884.
(43) Lim, J. H.; Yoon, J. H.; Kim, H. C.; Hong, C. S. *Angew. Chem., Int. Ed.* **2006**, *45*, 7424.
(44) Boudalis, A. K.; Sanakis, Y.; Clemente-Juan, J. M.; Mari, A.; Tuchagues, J.-P. *Eur. J. Inorg. Chem.* **2007**, 2409.

experimental and calculated behavior indicate that the relaxation process might be even more complex.

Conclusions

The ligand dpcp, employed in Ni^{II}/N_3^- chemistry, has fulfilled its promise to yield new complexes with new structural types and interesting properties. However in complex **1**, despite the heating used to induce methanolysis of the carbonyl function of the ligand, it is present in its carbonyl-hemiacetal form (i.e., only one carbonyl function underwent methanolysis). Direct current magnetic susceptibility studies showed the Ni^{II} ions are ferromagnetically coupled, yielding an $S = 5$ ground state. This finding is in agreement with the presence of end-on azide bridges, which promote ferromagnetic couplings. In addition, the cluster shows significant anisotropy of its ground state, which is a precondition for the emergence of single-molecule magnetism. Alternating current magnetic susceptibility experiments revealed clear out-of-phase signals, typical of SMMs, while field-sweep experiments showed a small but discernible hysteresis at 1.8 K. These results were also corroborated by the slow decay of the magnetization of **1** at 1.8 K, which was monitored in real time.

However, a careful inspection of the ac data revealed that (i) there seem to be at least two operative relaxation pathways and (ii) not all molecules exhibit slow magnetic relaxation. Conclusion (i) is inferred by the shape of the Cole−Cole plots between the real and imaginary parts of the ac susceptibility and by the shape of the χ_M' versus f curves at various temperatures, which showed two broad and overlapping peaks. Conclusion (ii) is inferred by the values of the χ_M'' maxima, which do not exceed 7.2% of the value expected ($0.5\chi_M$) of a sample in which all molecules exhibit slow magnetic relaxation.

In light of the trends in the literature of the field, a question will predictably arise: Is complex **1** an SMM? If an SMM is defined as a molecule that undergoes slow magnetic relaxation in the absence of long-range interactions, then a fraction of the molecules of **1** can be characterized as SMMs. But is **1** an SMM per se?

We would prefer to be cautious with the use of this term, which has been employed to describe a highly versatile phenomenon observed in a diverse variety of molecules. For this reason, we choose to simply describe **1** as a cluster with a high-spin ($S = 5$) ground state, of which a fraction of the molecules undergoes slow magnetic relaxation through at least two relaxation processes.

Acknowledgment. This work was supported by the Spanish Ministerio de Educación y Ciencia, project CTQ2006-15672-C05-03/BQC. We thank Dr. Yiannis Sanakis for helpful discussions during this work.

Supporting Information Available: Crystallographic data for **1** in CIF format, Figures S1 and S2 with error-contour plots for various J_1 versus J_2 combinations, Figure S3 with M versus HT^{-1} data for **1** along with an indicative fit. This material is available free of charge via the Internet at http://pubs.acs.org.

IC801441D